Nano-engineering PdNi networks by voltammetric dealloying for ethanol oxidation

Jieting Ding[1,2]·Shan Ji[1*]·Hui Wang[2*]·Bruno G. Pollet[3]·Rongfang Wang[2]

[1] College of Biological, Chemical Science and Chemical Engineering, Jiaxing University, Jiaxing, 314001, China

[2] College of Chemical Engineering, Qingdao University of Science and Technology, Qingdao, 266042, China

[3] Department of Energy and Process Engineering, Faculty of Engineering, Norwegian University of Science and Technology (NTNU), NO-7491 Trondheim, Norway

Corresponding Authors:

Shan Ji (*):jishan@mail.zjxu.edu.cn, Tel./fax: +86-573-82315109

Hui Wang (*): wangh@qust.edu.cn, Tel./fax: +86-13919839190.

Abstract:

PdNi particle networks (PdNi NN) are prepared by voltammetric dealloying using catkin-like PdNi nanoparticles as precursor. It is found that voltammetric dealloying plays an important role for the formation of these networks. Electron microscopy and X-ray diffraction are employed to show the evolution of the morphology of the as-prepared catalysts. The results generated from the cyclic voltammetry (CV) experiments showed that the PdNi NN was electrocatalytically active toward the ethanol oxidation reaction (EOR). Compared with PdNi/C and commercial Pd/C, the oxidation peak potential of PdNi NN shifted positively by +105 and +168 mV, and the peak current density increased by 1.53 and 3.75 times. The high electrocatalytic activity of PdNi NN toward the EOR afforded the feasibility to exploit highly active electro catalysts for direct ethanol fuel cells (DEFC).

Keywords: PdNi; Networks; Dealloy; Electrocatalyst, Ethanol oxidation

1. Introduction

Direct alcohol fuel cell (DAFC) is very well-suited for the transportation, military and portable power supply sectors due to its high-energy conversion efficiency, non-polluting credentials and several other advantages [1-3]. Palladium (Pd) has been demonstrated to be a promising platinum group metal (PGM) catalyst toward the ethanol oxidation in alkaline media, with Pd exhibiting a higher activity than platinum (Pt) [4]. However, the electrocatalytic oxidation of ethanol on Pd still needs to be further improved to meet the requirements of practical applications in DAFC [5]. An

effective method to achieve such catalytic improvement is to synthesize the precious metal as alloys. It is well-known that precious metal based alloys have excellent catalytic performances as fuel cell catalysts for the oxidation of small organic molecules [6]. It was found that the catalytic performance of metal alloy catalysts can be efficiently enhanced by adjusting their morphology, composition and structure [7]. Therefore, researchers prepared many alloy catalysts with high specific surface area, low density and high gas permeability [8-10]. For example, nano-flowered PdAg[11], nano-sponge-like PdPt[10] and porous nano-rod-like PdPt[12], all exhibit good electrocatalytic performances toward ethanol oxidation. However, these materials introduce surfactants during the preparation process, and the surfactants adsorbed on the surface of the metal alloy are difficult to remove [13].

In recent years, three-dimensional network metal catalysts have been widely concerned due to their high specific surface area, low density, high gas permeability and high density of atomic defects [14]. For example, Pd alloy material prepared by sol-gel method [15]. In addition, PtNi, PtNiP, PtCo, PdCoP and a series of alloy particle network catalysts have been prepared by ordinary chemical reduction methods [6, 14, 16-19]. These catalyst materials have focused on adjusting the elemental composition of network particles, demonstrating that bimetallic or multi-metal alloy catalysts can produce higher catalytic activity due to synergistic effects between different elements [20]. Recently, Pt-based alloy nanoparticles were prepared by dealloying transitional metal/Pt nanoparticles [16, 21]. It was found that the catalytic activity of the networked electrocatalyst can be improved by dealloying

the alloy precursors. On the other hand, the initial content of the transition metal in the alloy precursors should be sufficiently high and the particle size of the precursor must be sufficiently large [22, 23]. Therefore, to synthesize nano-scale networks, a suitable alloy precursor must be carefully selected.

In this study, we propose a novel and ´green´ method for synthesizing PdNi alloy with three-dimensional-network nanoparticles by electrochemical dealloying the catkin PdNi precursor. The precursor of PdNi particles is a cotton-like alloy, which is different from the dense solid alloy particles used in the previous reports [6, 14, 16]. This method could be extended to form other alloys with network-like structures, which are assembled by nanoparticles. Compared to the traditional acid treatment, in our novel process, electrochemical dealloying can gradually dissolve Ni; which is the key for the construction of a three-dimensional-network structure. After electrochemical cycling, the as-prepared PdNi network-like structure catalysts demonstrated higher electrocatalytic activity toward the EOR in alkaline solutions than those obtained for PdNi/C and commercial Pd/C catalysts.

2. Experiment

2.1 Synthesis

Analytical grade reagents and ultrapure water were used throughout the experiment. **Part One:** To prepare PdNi precursor, 0.6 mg $PdCl_2$ and 6 mg $NaBH_4$ were dissolved in 10 mL water respectively. pH of $PdCl_2$ solution was adjusted to 9 by adding 6 mol L^{-1} NaOH solution. With magnetic stirring and N_2 bubbling, the $NaBH_4$ solution was added dropwise to 30 mL of water contained 5 mg $NiCl_2 \cdot 6H_2O$, and then the $PdCl_2$

solution was rapidly added to the above solution. After continuously reacting for 30 minutes, the resultant precipitate was filtered and washed with ultrapure water. **Part Two:** To prepare the network structure PdNi alloy. The electrode carrying the precursor was cycled under cyclic voltammetry conditions in a N_2-saturated 0.1 mol L^{-1} $HClO_4$ electrolyte, at a scan rate of 50 mV s^{-1} and in the potential range of -0.2 to +1.0 V *vs.* Ag/AgCl.

2.2 Physical and Electrochemical Characterizations

X-ray diffraction (XRD) patterns of the as-prepared catalysts were recorded on a Shimadzu XD-3A diffractometer (Japan) using a filtered Cu Kα radiation. Transmission electron microscopy (TEM) measurement was carried out on a JEM-2010 Electron Microscope (Japan) with an acceleration voltage of 200 kV. The average chemical compositions of the as-prepared catalysts were determined using an IRIS Advantage inductively coupled plasma atomic emission spectroscopy (ICP-AES) system (Thermo, USA).

Electrochemical workstation potentiostat/galvanostat CHI 650D used to the electrochemical experiments of the catalysts. A representative three-electrode electrochemical cell was used all throughout the electrochemical testing in this study. For the electrochemical etching experiments, an Ag/AgCl (saturated KCl) electrode was used as reference (RE) electrodes. For the electrochemical measurements，a platinum wire and an Hg/HgO (1 mol L^{-1}KOH) electrode were used as the counter and reference electrodes respectively. A 5mm diameter glassy carbon disc as the working electrode (WE). The electrodes were prepared as follows: 2 mg of the

catalyst were dispersed in a 0.4 mL Nafion®/ethanol (0.25% Nafion®) solution. 8 μL of the dispersion was transferred onto the glassy carbon disc using a pipette. For CO stripping experiments, CO was adsorbed on the working electrode by bubbling the CO gas through the electrochemical cell for 10 min.

3. Results and Discussion

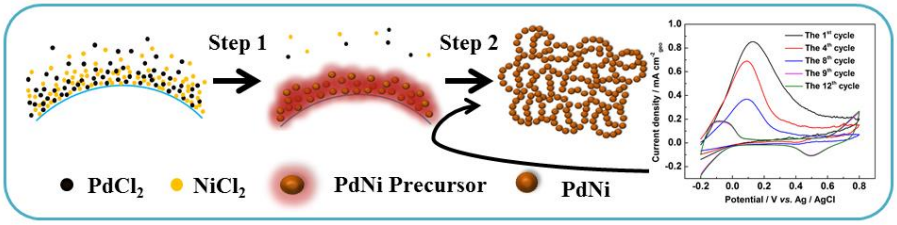

Fig. 1. Schematic of the synthesis method of PdNi and cycle voltammetry (CV) dealloying of PdNi.

The synthesis of the three-dimensional-network PdNi alloy is schematically illustrated in Fig. 1. The preparation process and methodology combine both ordinary chemistry and electrochemical etching. As an initial step, a new type of catkin precursor was prepared via a ´green´ method, and then followed by electrochemical etching. As the surface of Ni dissolved, a mesh PdNi catalyst was formed.

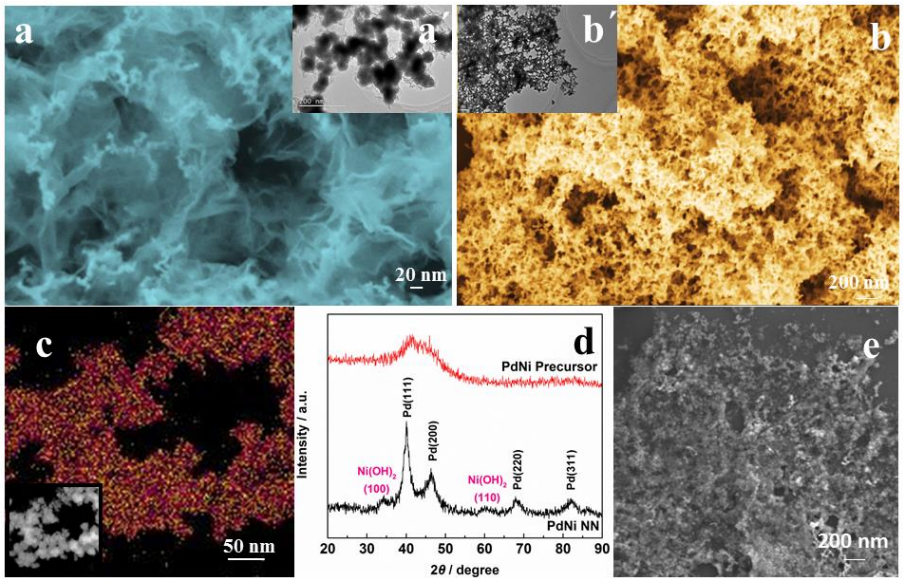

Fig. 2. (a; a´) SEM and TEM of PdNi precursors; (b; b´) SEM and TEM of PdNi NN; (c) EELS overlapped map of Pd (lavender) and Ni (orange) and the insets is show STEM images corresponding to EELS; (d) XRD patterns of PdNi precursor and PdNi NN catalysts; (e) SEM image of acid-treated sample.

SEM (Fig. 2(a)) and TEM (Fig. 2(a´)) images show that the PdNi precursor had catkin structures were ultrathin and wrapped in the surface of the nanoparticles. The X-ray diffraction (XRD) pattern for the PdNi precursor (Fig. 2(d)) confirmed the presence of an amorphous structure, because of the broad peak observed at $2\theta \approx 45°$ [7]. Then the work focused on the "Electrochemical etching" as a second step, in which cyclic voltammetry experiments were conducted as shown in Fig. 1. The synthesis process of the PdNi networks was carried out by cycling voltammetric dealloying in the potential range of -0.2 - +0.8 V *vs.* Ag/AgCl at a scan rate of 0.05 V s^{-1}. Fig. 1 shows the evolution of the CV change at various cycles. As shown in Fig. 1, a distinct oxidation peak in the first CV scan was observed due to the dissolution of surface Ni from the precursor surfaces. The first CV scan also indicates that the

precursor has a Ni-rich surface, which is in good agreement with our findings based on the SEM and TEM. As cycles continue, it can be observed that the Ni oxidation peak decreases, indicating a gradual removal of Ni atoms from the precursor, whilst the hydrogen desorption/absorption peaks can be clearly observed at the ninth cycle. The hydrogen desorption/absorption peaks and the metal oxidation/reduction peaks appeared, indicating that the Pd atoms formed on the surface were accompanied with a continuous dissolution of Ni atoms [24-26]. Based on the CV results, it was suggested that a two-step process exists during the formation of PdNi networks, as illustrated in the schematic in Fig. 1. These results show that the PdNi networks was formed after 9 cycles. The sample was collected after the 12th CV cycle for further testings to make sure the dealloying was fully completed.

The etched samples were then analyzed by SEM and TEM. Fig. 2(b) and 2(b′) show a network structure formed by the accumulation of nanoparticles. EELS element maps (Fig. 2(c)) show that the PdNi particles formed an alloy structure. As seen from Fig. 2(d), the sample exhibited six peaks. Pd formed a face-centered cubic (fcc) structure and had major peaks at around $2\theta \approx 40.0°$ (111), 46.5° (200), 68.1° (220), and 82.1° (311)[27]. The peaks at $2\theta \approx 34.3°$ and 60.5° are attributed to $Ni(OH)_2$ (100) and $Ni(OH)_2$ (110), respectively[28]. To further prove that the electrochemical etching produces a mesh structure, a control experiment was performed in which the PdNi precursor was directly immersed in a 0.1 mol L^{-1} $HClO_4$ solution for several hours. As the SEM image in Fig. 2(e) shows, the network structure was completely destroyed. Therefore, one may deduce that the electrochemical etching is the key to form a

network structure.

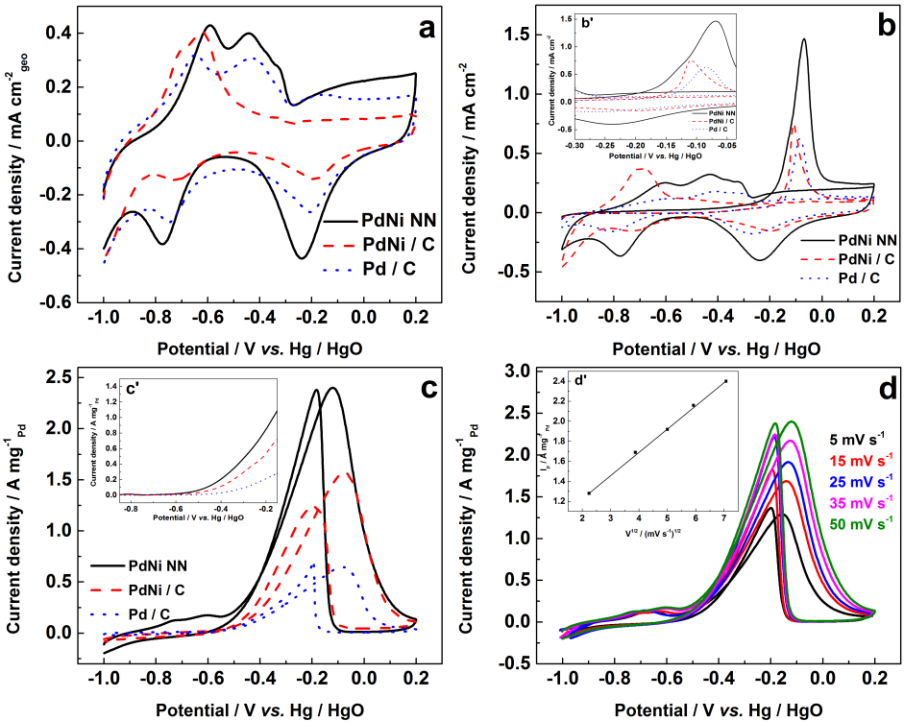

Fig. 3. (a) CV curves of PdNi NN, PdNi/C and Pd/C catalysts in 1.0 mol L^{-1} KOH. Scan rate: 50 mV s^{-1}; (b,b´) CO stripping voltammetry on electrodes in 1.0 mol L^{-1} KOH solution. Scan rate: 50 mV s^{-1}; (c) CV curves of catalysts recorded in 1.0 mol L^{-1} KOH + 1.0 mol L^{-1} C_2H_5OH solution. sweep rate: 50 mV s^{-1}; (c´) LSV curves for the three catalysts. Scan rate: 5 mV s^{-1}; (d) CV curve for EOR on PdNi NN at various sweep rates; (d´) I_p *vs.*$V^{1/2}$ plot.

Prior to electrochemical performance testing, PdNi/C samples were prepared by a simple method following reference[8]. Fig. 3(a) shows the cyclic voltammograms (CVs) of the three electro catalysts. In all CVs, a broad peak can be found in the lower potential region (from -0.83 to -0.35 V *vs.* Hg/HgO) on the forward scan, resulting from the OH^- adsorption on the surface of the catalysts. On the reverse scan, there is a defined peak around -0.25 V *vs.* Hg/HgO, which is characteristic of the reduction of

Pd oxide to Pd. The study of CO-stripping was shown in Fig. 3(b). It can be observed that the adsorbed CO was oxidized completely in the first (1st) scan, and no CO oxidation was observed during the second (2nd) scan on all three catalysts. The CO-oxidized onset potentials were also presented as inset in Fig. 3(b). The figure clearly shows that the onset potentials of CO oxidation follow the order: Pd/C < PdNi/C < PdNi NN. Fig. 3(c) shows the EOR CVs of the three catalysts. The value of the peak current density of the as-prepared PdNi NN was found to be 2.4 A mg^{-1}_{Pd}, which is 1.53 and 3.75 times greater than that of the PdNi/C (1.56 A mg^{-1}_{Pd}) and Pt/C (0.64 A mg^{-1}_{Pd}) respectively. In our conditions, effective EOR catalysts exhibited lower EOR onset potentials. Fig. 3(c′) shows the EOR onset potentials measured by Linear Sweep Voltammetry (LSV) on the three catalysts. PdNi NN exhibits the lowest onset potential (-0.590 V *vs.* Hg/HgO) among the three catalysts, which are 105 and 168 mV more negative than that of PdNi/C (-0.485 V *vs.* Hg/HgO) and Pd/C (-0.422 V *vs.* Hg/HgO) respectively. Among the three catalysts, PdNi NN produced the highest EOR catalytic activity in terms of peak current density and low EOR onset potentials, indicating that the electrochemical etching yielded a three-dimensional network catalyst with the highest mass activity. Fig. 3(d) is CV curves of ethanol oxidation on PdNi NN at various sweep rates. It can be seen from the figure that as the sweep rate increases, the peak current density (I_p) and peak potential of ethanol oxidation are positively shifted. I_p linearly increases with the square root of sweep rate ($V^{1/2}$) in the range of 5-50 mV s^{-1} (Fig. 3(d')), indicating that the reaction is controlled by diffusion, rather than surface electron transfer kinetics.

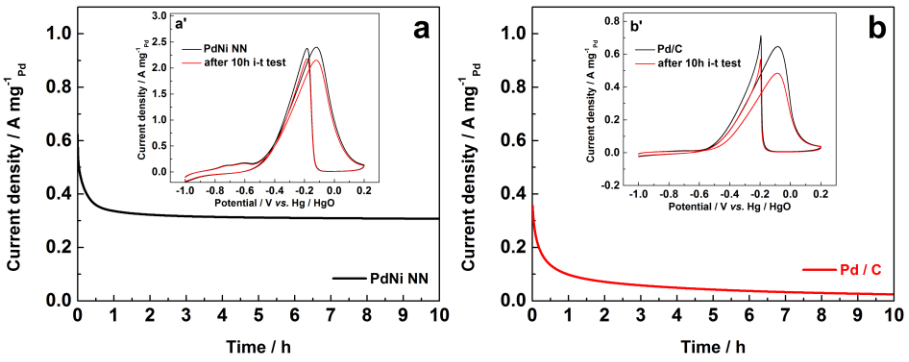

Fig. 4. (a,b) Chronoamperometry (CA) curves of the catalysts recorded in 1.0 mol L^{-1} KOH + 1.0 mol L^{-1} C_2H_5OH solution; potential: -0.3 V *vs.* Hg/HgO; (a´,b´) CVs obtained for durability analysis derived after i-t test.

Fig. 4 is CA curves of PdNi NN and commercial Pd/C in a saturated solution of 1.0 mol L^{-1} C_2H_5OH and 1.0 mol L^{-1} KOH with a fixed potential (-0.3 V *vs.* Hg/HgO) for a duration of 10 hours. It can be seen from the Fig. 4(a, b) that PdNi NN has a higher EOR current density (0.31 A mg^{-1}_{Pd}) than Pt/C after 10-hour testing. The insets of Fig. 4 show that the mass activity of PdNi NN decreased from 2.4 A mg^{-1}_{Pd} to 2.14 A mg^{-1}_{Pd} after the i-t test. In other word, the mass activity of PdNi NN drops about 11%. However, the mass activity of Pd/C decreased from 0.64 A mg^{-1}_{Pd} to 0.48 A mg^{-1}_{Pd}, and drops about 25%. Therefore, PdNi NN has better stability in EOR than commercial Pd/C.

4. Conclusions

Using catkin alloy precursors to prepare three-dimensional-network PdNi nanoparticles by electrochemical cycling was presented in this study. During the etching process, the PdNi nanoparticles were assembled to form a network in which the dissolution of Ni occurred steadily upon electrode cycling. It is worth noting that

the formation of the network structure strongly depends upon the etching method when compared to acid treatment. Compared with previous PdNi/C and commercial Pd/C data on the EOR, the as-prepared PdNi NN catalyst exhibited better catalytic activity as well as durability. It was found that the obtained PdNi networks could be a potential candidate as a Direct Ethanol Fuel Cell catalyst.

Acknowledgements

The authors would like to thank the National Natural Science Foundation of China (21766032 and 51661008) and Shenzhen Innovation Fund (JCYJ20160520161411353) for financially supporting this work.

References

[1] S.T. Nguyen, H.M. Law, H.T. Nguyen, N. Kristian, S. Wang, S.H. Chan, X. Wang, Applied Catalysis B: Environmental, 91 (2009) 507-515.
[2] L. Chen, H. Guo, T. Fujita, A. Hirata, W. Zhang, A. Inoue, M. Chen, Advanced Functional Materials, 21 (2011) 4364-4370.
[3] U.B. Demirci, Journal of Power Sources, 169 (2007) 239-246.
[4] Q. Yi, F. Niu, L. Sun, Fuel, 90 (2011) 2617-2623.
[5] J. Yin, S. Shan, M.S. Ng, L. Yang, D. Mott, W. Fang, N. Kang, J. Luo, C.J. Zhong, Langmuir : the ACS journal of surfaces and colloids, 29 (2013) 9249-9258.
[6] R. Wang, Y. Ma, H. Wang, J. Key, S. Ji, Chemical communications, 50 (2014) 12877-12879.
[7] Y. Ma, R. Wang, H. Wang, V. Linkov, S. Ji, Physical chemistry chemical physics : PCCP, 16 (2014) 3593-3602.
[8] H. Yang, H. Wang, H. Li, S. Ji, M.W. Davids, R. Wang, Journal of Power Sources, 260 (2014) 12-18.
[9] H.L. Liu, F. Nosheen, X. Wang, Chemical Society reviews, 44 (2015) 3056-3078.
[10] C. Zhu, S. Guo, S. Dong, Chemistry, 19 (2013) 1104-1111.
[11] W. Hong, J. Wang, E. Wang, Electrochemistry Communications, 40 (2014) 63-66.
[12] Y. Lu, Y. Jiang, W. Chen, Nano Energy, 2 (2013) 836-844.
[13] J. Wang, X.B. Zhang, Z.L. Wang, L.M. Wang, W. Xing, X. Liu, Nanoscale, 4 (2012) 1549-1552.
[14] L. Zhang, D. Lu, Y. Chen, Y. Tang, T. Lu, J. Mater. Chem. A, 2 (2014) 1252-1256.
[15] A.-K. Herrmann, P. Formanek, L. Borchardt, M. Klose, L. Giebeler, J. Eckert, S. Kaskel, N. Gaponik, A. Eychmüller, Chemistry of Materials, 26 (2013) 1074-1083.
[16] Y. Xu, Y. Yuan, A. Ma, X. Wu, Y. Liu, B. Zhang, Chemphyschem : a European journal of chemical physics and physical chemistry, 13 (2012) 2601-2609.
[17] Y. Ma, H. Wang, W. Lv, S. Ji, B.G. Pollet, S. Li, R. Wang, RSC Advances, 5 (2015) 68655-68661.

[18] H. Li, Y.-J. Li, L.-L. Sun, X.-L. Zhao, Electrochimica Acta, 108 (2013) 74-78.
[19] W. Liu, A.K. Herrmann, D. Geiger, L. Borchardt, F. Simon, S. Kaskel, N. Gaponik, A. Eychmuller, Angewandte Chemie, 51 (2012) 5743-5747.
[20] Q. Wan, Y. Liu, Z. Wang, W. Wei, B. Li, J. Zou, N. Yang, Electrochemistry Communications, 29 (2013) 29-32.
[21] J. Xu, G. Fu, Y. Tang, Y. Zhou, Y. Chen, T. Lu, Journal of Materials Chemistry, 22 (2012) 13585.
[22] J. Snyder, I. McCue, K. Livi, J. Erlebacher, Journal of the American Chemical Society, 134 (2012) 8633-8645.
[23] M. Oezaslan, M. Heggen, P. Strasser, Journal of the American Chemical Society, 134 (2012) 514-524.
[24] J. Ding, S. Ji, H. Wang, J. Key, D.J.L. Brett, R. Wang, Journal of Power Sources, 374 (2018) 48-54.
[25] J. Ding, S. Ji, H. Wang, B.G. Pollet, R. Wang, Electrochimica Acta, 255 (2017) 55-62.
[26] R. Wang, H. Wang, F. Luo, S. Liao, Electrochemical Energy Reviews, 1 (2018) 324-387.
[27] S. Yang, X. Zhang, H. Mi, X. Ye, Journal of Power Sources, 175 (2008) 26-32.
[28] D. Ghosh, S. Giri, A. Mandal, C.K. Das, Chemical Physics Letters, 573 (2013) 41-47.